U.S. Department of the Interior

Geological Survey

HEAT FLOW FROM THE WESTERN ARM OF THE BLACK ROCK DESERT, NEVADA

by

C. W. Mase and J. H. Sass

U.S. Geological Survey Open-File Report 80-1238

1980

This report is preliminary and has not been reviewed for conformity
with U.S. Geological Survey editorial standards and stratigraphic nomenclature.

Abstract

Heat-flow values for 12 new sites in the western Black Rock Desert range from 56 mWm^{-2} to over 500 mWm^{-2} near Double Hot Springs. Combining these results with over 20 values obtained by Sass and others (1979) yields a mean heat flow of 76 ± 4 mWm^{-2} outside of the areas of anomalous heat flow associated with thermal spring systems. This mean is significantly lower than that characteristic of the Battle Mountain heat-flow high (>125 mWm^{-2}) and is of doubtful regional significance because of the observed hydrothermal phenomena and because some of the recharge for the systems may originate within the basin. The lack of recent volcanism in the region and the apparently normal Basin and Range heat flow suggests that geothermal systems are stable stationary phases supported by high regional heat flow with the fluid flow governed by the configuration of fractures and permeable formations and forced by a regional piezometric gradient controlled by topography and precipitation.

The complexity of the heat-flow pattern probably arises from hydrothermal circulation supporting the numerous hot springs throughout the region. Upward groundwater flow from depths of from 2 to 6 km can maintain the temperatures that are observed for hot springs in the western Black Rock Desert. Microearthquake activity indicates active fracturing to the required depths of circulation. The net anomalous heat discharge from the hot spring systems is estimated at 34 MW based on convective and conductive heat loss. Steady-state heat transfer by moving groundwater in a normal Basin and Range heat-flow environment can easily provide the observed power loss.

INTRODUCTION

Hydrothermal activity occurs at many locations along the margins of the Black Rock Desert in northern Nevada (Waring, 1965; Renner and others, 1975; Brook and others, 1979). The youngest volcanism in the region is basaltic and has been dated at 23 m.y. (Grose and Sperandio, 1978), too old to represent heat sources for the modern hydrothermal activity. On the basis of high thermal gradients in wells, high heat flow in contiguous regions and the observed hydrothermal activity, Sass and others (1979, 1980) and Lachenbruch and Sass (1977, 1978) have included the Black Rock Desert within the Battle Mountain heat-flow high (BMH, Figure 1). This suggests that geothermal systems within the Black Rock Desert may be the result of deep circulation of groundwater, storage, and heating within a reservoir due to a high regional heat flow with subsequent discharge to the surface through permeable conduits within fault zones.

The present work was undertaken to provide additional heat-flow information for a geothermal resource assessment of the western arm of the Black Rock Desert. The assessment is primarily the responsibility of the Water Resources Division (WRD) of the U.S. Geological Survey and the Bureau of Land Management (BLM). All of the new data discussed herein were obtained from holes sited and drilled by WRD (Alan H. Welch, personal communication, 1980; Schaefer and others, 1980). We have combined the data from 12 new heat-flow sites (Figure 2) with the results of Sass and others (1979) in an attempt to determine the thermal structure of the western Black Rock Desert, to delineate the extent of subsurface thermal features and to ascertain the nature and origins of the thermal fluids and heat sources.

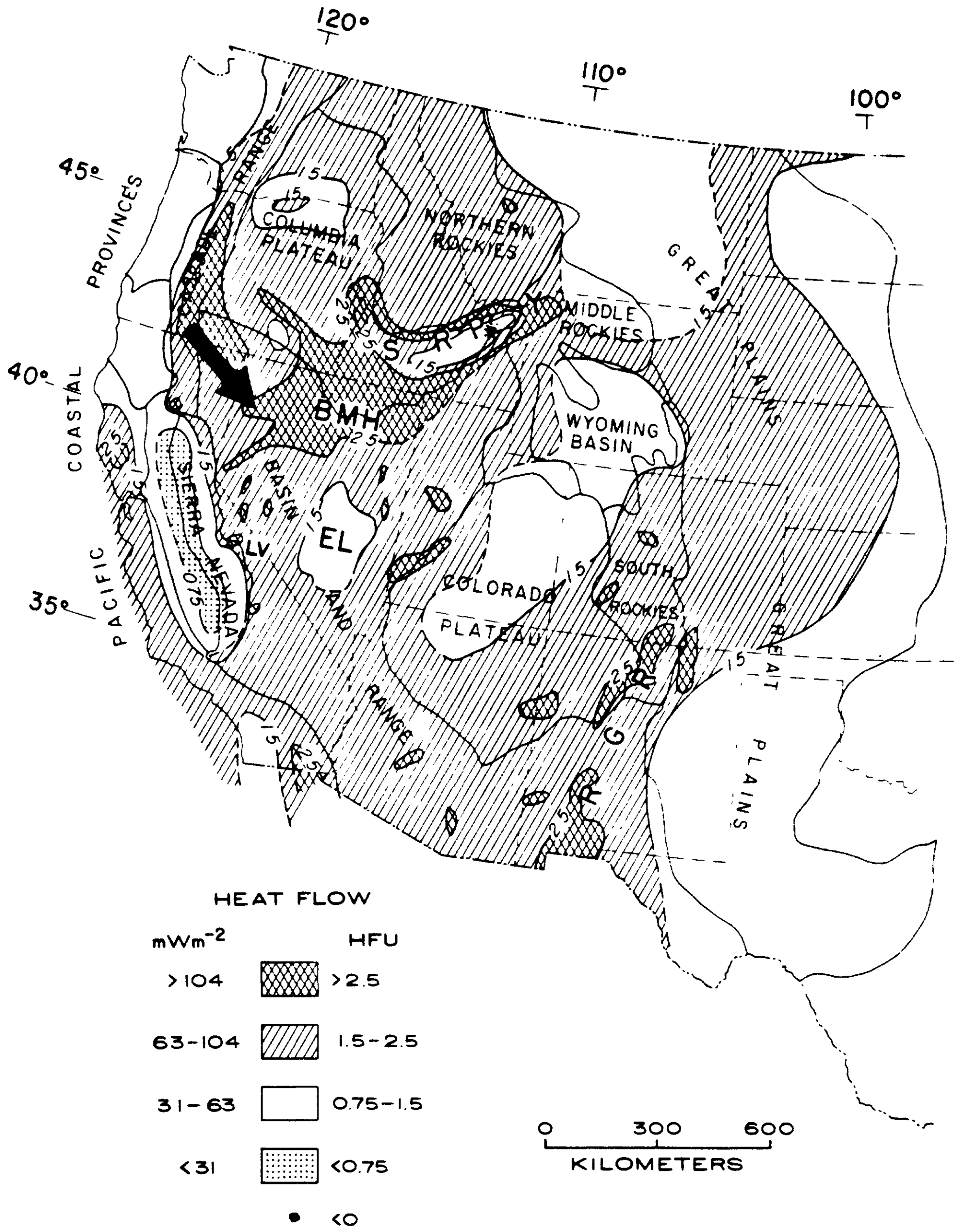

Figure 1. Generalized map of heat flow and physiographic provinces in the western U.S. (after Lachenbruch and Sass, 1978; Lachenbruch, 1978). Abbreviations are BMH, Battle Mountain High; SRP, Snake River Plain; IB, Idaho Batholith; Y, Yellowstone; RGR, Rio Grande Rift; EL, Eureka Low; LV, Long Valley. Arrow indicates present study area.

The following symbols and units are used in the remainder of this report:

T, temperature, °C

K, thermal conductivity, W $m^{-1}K^{-1}$; 1 HCU (mcal $cm^{-1}s^{-1}°C^{-1}$) = .418 W m^{-1} K^{-1}

z, depth, m positive downwards

v_z, vertical (seepage) velocity m s^{-1} or mm y^{-1} or volume flux of water

Γ, vertical temperature gradient, °C km^{-1} or K km^{-1}

q, vertical conductive heat flow, mWm^{-2} or kW km^{-2}, or HFU (10^{-6} cal cm^{-1} s^{-1}): 1 HFU = 41.8 mW m^{-2}

Acknowledgments. The comments of Art Lachenbruch and Allen Welch were particularly helpful in the development of this paper. We thank Pete Galanis for preparation of the geologic sketch map used in Figures 2, 4, and 5.

GEOLOGIC SETTING

The western arm of the Black Rock Desert occupies a position near the western margin of the Basin and Range physiographic province. The region is characterized by roughly parallel mountain ranges and basins having a north-northeast trend. The region is one of currently active tectonism marked by abundant late Pleistocene and Holocene faults. The major hot springs in the area, Black Rock Point, Double, Fly Range, Gerlach, Mud and Trego, occur on or very near faults with Quaternary displacements. Surficial tension cracks (interpreted as tectonic in origin, Grose, 1978), fault patterns and seismic focal mechanisms indicate active tectonic spreading along a WNW-ESE axis in the western Black Rock Desert region (Kumamoto, 1978). This pattern is consistent with a relatively uniform WNW-ESE extension direction throughout northern Nevada (Zoback and Thompson, 1978). The geologic setting of the western Black Rock Desert is summarized in Figure 2. The geologic information in the figure is generalized from Grose and Sperandio (1978), Bonham (1969), and Wilden (1964).

The ranges surrounding the western Black Rock Desert are composed largely of Cretaceous granodiorite, Permo-Triassic meta-volcanic and meta-sedimentary rocks and late Oligocene - early Miocene rhyolitic, andesitic, and basaltic sequences. Valley fill includes late Tertiary and Quaternary fluviatile and lacustrine sediments that were deposited concurrently with normal faulting.

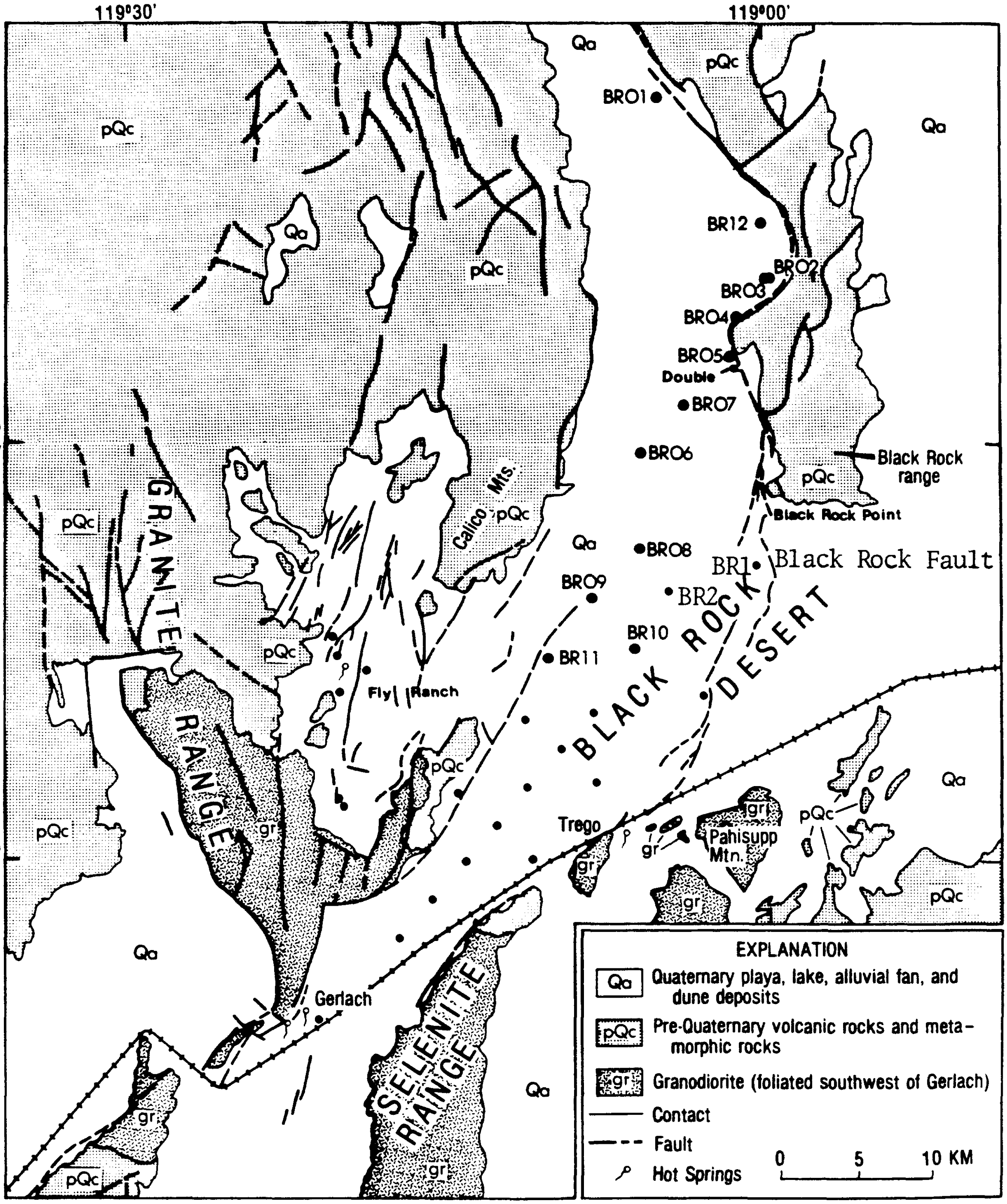

Figure 2. Geologic sketch map of the western Black Rock Desert and adjoining ranges. Geology and faults generalized from Grose and Sperandio (1978), Bonham (1969), and Wilden (1964). Small dots indicate control from Sass and others (1979).

GEOTHERMAL GRADIENT AND HEAT-FLOW DATA

The most recent temperature-depth profiles for 12 new heat-flow sites in the southern Black Rock Desert are shown in Figure 3. Based on thermal considerations, Lachenbruch and others (1976) have suggested the thermal gradient profiles for areas within or near hydrothermal systems be divided up into three distinct groups. The three groups are considered to be characteristic of regions with hydrologic recharge (Group I), regions with conductive regimes to substantial depths (Group II) and regions of hydrologic discharge (Group III). Group I boreholes (BR06 through BR11, Figure 3) yield significantly low gradients (53 to 85 °C km^{-1} compared to an expected gradient of ∿120 °C km^{-1} for the playa if the heat flow is indeed characteristic of the BMH) suggesting that heat from below is being absorbed by downward movement of water, a condition characteristic of hydrologic recharge. The upper parts of the temperature profiles from these boreholes show the influence of upward water movement probably due to discharge from a shallow subsystem within the playa sediments. Group II boreholes (BR01 and BR04, Figure 3) yield a gradient and heat flow comparable to the hydrologically undisturbed regional value (∿125 mWm^{-2}), suggesting that heat transfer is accomplished primarily by conduction. Group III boreholes (BR02, BR03, BR05, and BR12, Figure 3) have thermal gradients that are generally quite large and variable with depth, a characteristic influence of upward and/or lateral convection of thermal fluids through fracture zones or vertically permeable formations. The high-frequency excursions in the temperature profiles for boreholes BR10 and BR11 are attributed to the presence of gas bubbles observed streaming from the borehole during logging.

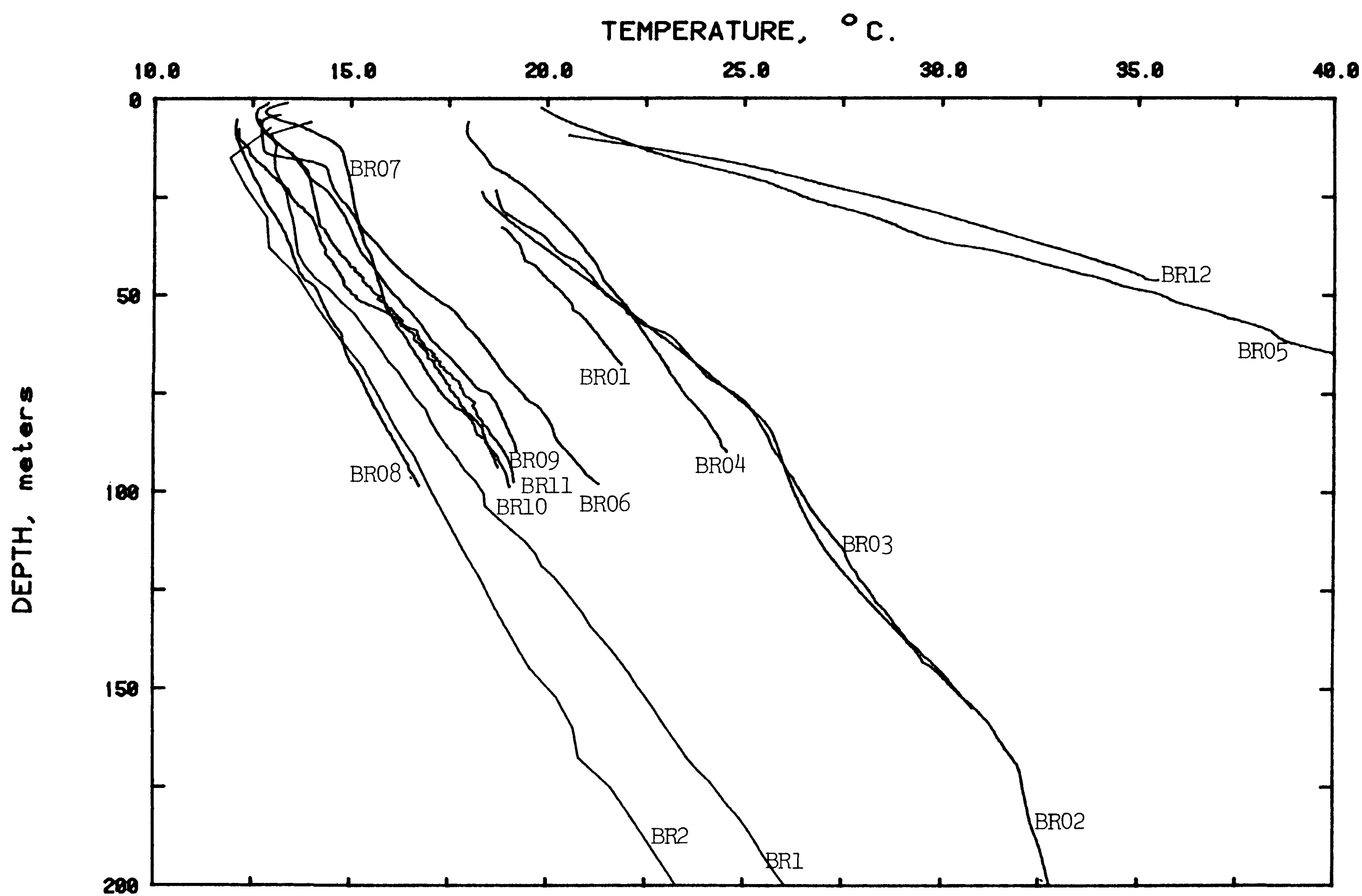

Figure 3. Temperature profiles for USGS wells BR01 through BR12, Black Rock Desert.

Heat-flow data for the 12 new sites are summarized in Table 1. The vertical component of heat flow, q, was computed as the product of the harmonic mean thermal conductivity, $\langle K \rangle$, and the least-squares temperature gradient, Γ, over each linear section of the temperature profile. Solid component thermal conductivities, K_s, were measured from chips in a divided-bar apparatus following the methods described by Sass and others (1971). To determine the formation or in situ conductivity, K_r, the measured conductivity of the solid component must be combined with an estimate of formation porosity, ϕ. From measurements on cores from other localities in the Northern Great Basin, we adopted a value for ϕ of 0.3 ± 0.1 and calculated in situ conductivities using the geometric mean (i.e., $K_r = K_s^{(1-\phi)} K_w^{\phi}$, where K_w is the thermal conductivity of water). For boreholes drilled into playa sediments, an average conductivity of 1.05 W m^{-1} K^{-1}, determined in situ by Sass and others (1979), was used. Assigning a single gradient to boreholes exhibiting the effects of lateral and vertical water movement, for the purpose of calculating a conductive heat loss, is somewhat arbitrary. In general, the most linear section of the near-surface temperature-depth curve was used to calculate the least-squares gradient. The resulting conductive heat loss obtained is of little regional significance but is useful in determining the nature and origins of thermal fluids and heat sources for the numerous spring systems.

Heat-flow values for the 12 new sites range from 56 mW m^{-2} to over 500 mW m^{-2} (near Double Hot Springs). Combining these results with results from Sass and others (1979) yields a mean heat flow of 76 ± 4 mW m^{-2} outside of the areas of anomalous heat flow associated with thermal spring systems. This mean is significantly lower than that characteristic of the Battle Mountain

TABLE 1. Locations, conductive temperature gradients, lithologies, conductivities, and estimated heat flows for holes in the northern Black Rock Desert

Borehole	N. Lat.	W. Long.	Elev. (m)	Depth range (m)	Γ (°K km^{-1})	Type Γ†	Lithology	Conductivity¶ (Wm^{-1} K^{-1})	q (mWm^{-2})
BR01	41° 12.3'	119° 3.8'	1250	30-68	88.00 (.46)	c	alluvium	1.22 (.13)	107 (12)
BR02	41° 5.9'	118° 59.5'	1250	30-76	121.8 (.6)	c	alluvium	1.29 (.14)	157 (18)
				76-171	76.50 (.35)	d,c	alluvium	1.29 (.14)	99 (11)
				171-228	27.20 (.14)	d,c	Ter. vol.	1.84 (.14)	50 (4)
BR03	41° 5.9'	118° 59.6'	1250	30-85	127.7 (.29)	c	alluvium	1.29* (.14)	165 (18)
				85-155	50.90 (.68)	d,c	alluvium	1.29* (.14)	67 (8)
BR04	41° 4.5'	119° 1.1'	1219	40-90	70.92 (.18)	c	alluvium	1.34 (.15)	95 (11)
BR05	41° 3.1'	119° 1.4'	1215	15-76	356 (1)	d,c	alluvium	1.19 (.13)	423 (47)
				76-189	225 (1)	d,c	alluvium	1.41 (.18)	318 (42)
				189-215	115 (1)	d,c	Ter. vol.	2.17 (.51)	250 (61)
BR06	40° 59.6'	119° 6.0'	1204	55-99	82.15 (.39)	c	clay	1.05** (.05)	86 (5)
BR07	41° 1.3'	119° 3.8'	1205	55-99	76.71 (.69)	c,r	clay	1.05** (.05)	81 (5)
BR08	40° 56.2'	119° 5.9'	1180	15-98	53.78 (.11)	c	clay	1.05** (.05)	56 (3)
BR09	40° 54.4'	119° 8.3'	1180	40-90	85.57 (.52)	c,d,r	clay	1.05** (.05)	90 (5)
BR10	40° 52.7'	119° 6.2'	1185	58-94	67.13 (.39)	c,r	clay	1.05** (.05)	70 (4)
BR11	40° 52.4'	119° 10.1'	1190	34-96	81.80 (.50)	c	clay	1.05** (.05)	86 (5)
BR12	41° 7.9'	119° 0.0'	1235	9-46	386 (4)	d	alluvium	1.34*** (.18)	517 (75)

†Type of Γ: c = conductive regime; d = discharge and/or upward movement of water; r = recharge and/or downward movement of water.

¶Conductivities were estimated on the basis of the harmonic mean of the solid component, $\langle K_s \rangle$, as measured from drill cuttings using the "chip" method (Sass and others, 1971). A correction has been applied for formation porosity (see text).

*Conductivities estimated from measurements in adjacent borehole, BR02.

**Average conductivity (1.05 Wm^{-1} °K^{-1}) determined in situ for playa sediments in the southern Black Rock Desert, Nevada (Sass and others, 1979a, 1979b).

***Conductivity estimated from BR04 of similar type locality.

heat-flow high ($\sim$125 mW m^{-2} or $\sim$3 HFU, see Figure 1). The average of 76 mWm^{-2} certainly is not indicative of the total heat loss from the region because of the observed hydrothermal manifestations and because some of the recharge for the systems may originate within the basin.

DISCUSSION

The addition of 12 new heat-flow sites in the Black Rock Desert does not significantly alter the interpretation of Sass and others (1979). Our interpretation of heat-flow data combined with the interpretation of Sass and others (1979) reveals a complex pattern of heat flow probably arising from hydrothermal circulation supporting the numerous hot springs throughout the region. The heat-flow contours (Figure 4) may be compared with the depth-to-basement contours (Figure 5). It is noteworthy that the two areas of lowest heat flow coincide with the areas of lowest topography and the deepest parts of the basin. The regions of high heat flow associated with hot spring systems are in every instance related to a range-bounding fault. The most poorly controlled and most speculative thermal anomalies are those associated with the Holocene Black Rock fault (Dodge, 1979). Here we have three separate, high heat-flow values with little spatial control of the anomalies. In spite of the limited spatial coverage, we have drawn in heat-flow contours based on surface geology and hot spring locations. Thus, there is considerable latitude in drawing the contours along the Black Rock fault (Figure 4), and we might expect significant changes to our tentative interpretation with improvement in the control.

A rough calculation of the power loss for geothermal systems yields insight into the nature and origins of the thermal fluids and heat sources. The total power loss for hydrothermal systems in the Black Rock Desert may be estimated from the combined anomalous conductive heat loss over the systems and adding to this the enthalpy of the discharge waters. In Table 2, we have summarized the various estimates of spring discharge and discharge temperatures. This yields a combined convective loss of 8.4 MW. Using a conservative multiplier of 3 (cf. Olmsted and others, 1975; Mase and

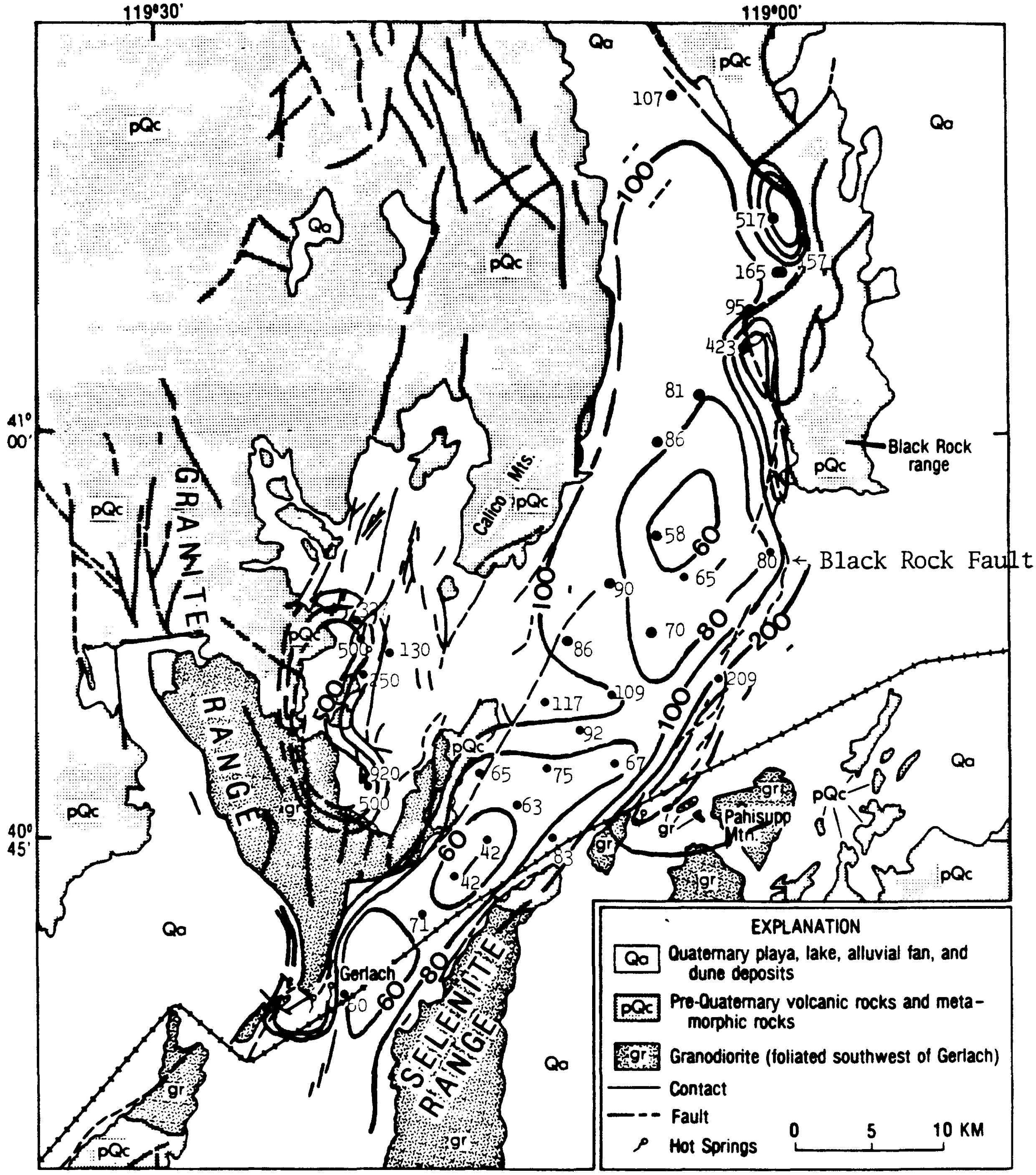

Figure 4. Heat-flow contours (60, 80, 100, 200, 300, 500 mW m^{-2}), western Black Rock Desert. Major normal faults also indicated (modified from Sass and others (1979)).

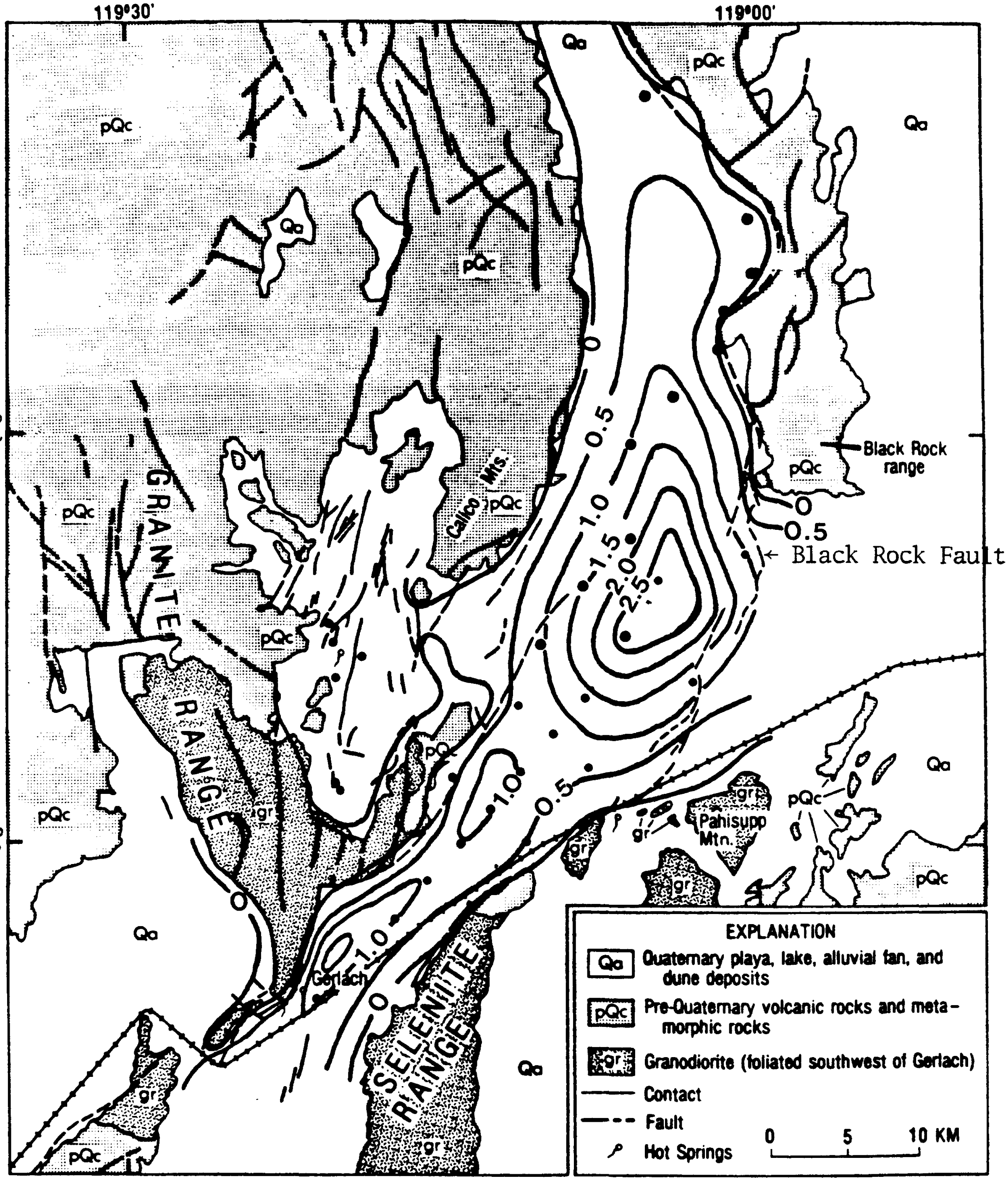

Figure 5. Depth to basement in the western Black Rock Desert (generalized from Crewdson, 1978, and Schaefer and others, 1980). Contours labeled in kilometers. Location of heat-flow points shown for reference.

TABLE 2. Estimates of heat discharge for hot springs in the southern Black Rock Desert

Site	Reference	Surface Temp. (T_s)	Discharge (kg sec^{-1})	$\Delta T = T_s - T_m^*$	Heat Discharge = $\rho_f C_f \cdot \Delta T \cdot$ [Discharge] (Mw)
Gerlach/Great Boiling Hot Springs	Olmsted and others, 1975	80°	16.7	69	5.0
Double Hot and Black Rock Point	Renner and others, 1975	80°	2.9	69	0.8
Trego	Waring, 1965	84°	1.3	73	0.4
Fly Ranch	Brook and others, 1979	80°	8.3	69	2.2
TOTAL			29.2		8.4

*Mean annual temperature = 11°C

† ρ_f = density = $.97 \times 10^3$ kg/m³

others, 1978) for the anomalous conductive loss, we estimate a combined heat loss (above background) of ∿34 MW for hydrothermal systems of the Black Rock Desert. If the anomalous heat discharge is supported entirely by the enthalpy of the thermal waters, assuming a mean annual temperature of 11°C in the recharge areas and a temperature of 150°C for the thermal fluids leaving the deep source (estimated average from silica reservoir temperatures, Anderson, 1978; Mariner and others, 1974), then a minimum mass discharge of 60 kg sec^{-1} is required of the hydrothermal systems. For this mass discharge rate 29 kg sec^{-1} is vented at the surface in the form of hot springs, with the remainder being discharge from the reservoir into shallow aquifers, the heat being lost conductively.

Keller and others (1978) interpret the hydrothermal regime of the southern Black Rock Desert in terms of thermal blanketing by low conductivity sediments in a "normal" Basin and Range geothermal regime. Using chemically inferred reservoir temperatures for the spring systems and the depths of the alluvial cover, they estimate a mean thermal gradient of 140 °C km^{-1} on the assumption that springs are sampling aquifers near the base of the adjacent alluvial fill. This gradient would yield a regional heat flow of 145 mW m^{-2}, a value characteristic of some of the hotter parts of the Battle Mountain heat-flow high (Sass and others, 1971, 1977; Lachenbruch and Sass, 1977). According to the heat-flow data (Figure 4), the deeper parts of the valley are quite cold suggesting that thermal blanketing by low conductivity sediments is playing a relatively minor role in the heating of reservoir fluids.

The fact that the lowest observed heat flows coincide with the lowest topography and deepest parts of the basin strongly suggest that fluid movement within the basin represents part of the recharge for the hydrothermal systems. It is possible that the piezometric surface within the valley declines with elevation and that a downward piezometric gradient exists over much of the lowland area. If we can make an estimate of the downward water velocity (volume flux of water), then we may also estimate the amount of possible recharge contributed by the basin. Supposing that the groundwater percolates downward uniformly, then the average vertical groundwater velocity in the playa sediments is given by

$$V_z = \frac{K}{\rho_f C_f L_o} \ln \left(\frac{qb}{qs}\right) \tag{1}$$

(modified from equation 10 of Lachenbruch and Sass, 1977) where K is the thermal conductivity of the sediments, ρ_f and C_f are the density and specific heat of the fluid phase respectively, L_o is the characteristic depth of circulation and qb and qs are heat fluxes into the base and out of the surface respectively. For an observed conductivity for playa sediments of 1.05 Wm^{-1} $°K^{-1}$ (Sass and others, 1979), an average surface heat flux of 72 mW m^{-2} (area <100 mW m^{-2}) and assuming a depth of circulation on the order of the average depth to basement (1.5 km from Figure 5) and a basal heat flux of 125 mW m^{-2}, characteristic of the Battle Mountain high, equation (1) yields a downward velocity of ~3 mm yr^{-1} (~10^{-10} m sec^{-1}) within the basin fill. This velocity integrated over the area of low heat flow (<100 mW m^{-2}, Figure 3) results in a maximum recharge of 36 kg sec^{-1}, some 60% of the required mass discharge necessary to support the hydrothermal systems. An average depth of circulation of 1.5 km is required to obtain the mean inferred reservoir temperature of 150°C predicted from silica geothermometry. Furthermore, the average heat-flow anomaly, relative to the Battle Mountain High, is ~50 mW m^{-2} over the basin. This results in a contribution of ~20 MW or approximately 55% of the total estimated heat loss of

34 MW, when integrated over the area of low heat flow. The uncertainties in these calculations are such that convection within unconsolidated playa sediments could account for all of the observed mass discharge and heat loss of the spring systems.

The permeabilities of the fault zones through which thermal fluids rise are not known. However, if we consider an average of 5 darcies (Sorey, 1975) for the permeable part of the fault zone, a vertical piezometric gradient of $\sim$1% is required to account for the mass discharge of the spring systems. The boreholes located on the playa (BR1, BR2, and BR06-BR11, Figures 2 and 3) have an extrapolated mean annual temperature $\sim$5°C lower than the mean annual temperature for boreholes located off the playa (BR01-BR05, and BR12, Figures 2 and 3). This difference in albedo, attributed to the lack of vegetation on the playa, results in a piezometric gradient of $\sim$1% (buoyancy effect caused by a ΔT of 5°C over a column of water) between fluids within the playa and fluids contained within fault zones adjacent to the playa. Thus, the driving forces for the spring systems could result from free convection initiated by a change in surface albedo.

This crude analysis, while sensitive to some rather tenuous assumptions regarding the ratio of conductive to convective heat flux, reservoir temperature, depth of circulation and size of the systems (among others) suggests that 60% to 100% of the systems mass discharge and heat loss may be accomplished by slow downward percolation of groundwater through playa sediments into a porous and permeable basal alluvium unit, from which the thermal fluids can move laterally and be subsequently discharged to the surface through fault zones, with the driving force supplied by the density contrast in the recharge versus discharge columns.

It should be further noted, however, that the observed low heat flows could just as easily reflect a thermal boundary imposed by lateral water flow in a porous and permeable alluvium unit beneath the playa clays. In this case, circulation of meteoric waters within playa sediments is playing a minor role in the heating of reservoir fluids. This, in turn, suggests that the thermal spring systems in the region are maintained solely by deep circulation of metoric waters within the crystalline basement of the surrounding ranges. Only one or more deep boreholes through the basin fill into the crystalline basement will be able to resolve this ambiguity.

If we assume that the basin plays a minor role in the heating of thermal fluids, then the heat and mass discharge in the vicinity of the springs must be balanced by recharge occurring in the surrounding ranges. The anomalous heat discharge from the spring systems is equivalent to the regional heat flow (125 mW m^{-2} or 3 HFU, Figure 1) over 275 km^2. If recharging groundwater absorbs 30% to 60% of the regional heat flow as is the case for Roosevelt Hot Springs, Utah, (Ward and others, 1978), heat absorbed over a recharge area of 400 to 900 km^2 could maintain the observed power loss. The ranges surrounding the Black Rock Desert (Granite, Black Rock, and Selinite Ranges, Figure 1) constitute more than sufficient area for recharge. The groundwater may also absorb a substantial amount of heat in lateral movement to the hot storage "reservoir". Supposing that the groundwater percolates downward uniformly, then vertical groundwater velocities in the recharge zones required to sustain the mass discharge rate range from 2 to 4 mm yr^{-1} (30% and 60% heat absorption, respectively), some 1% to 2% of the local annual precipitation within the ranges. For these recharge velocities, the depth of water flow needed to achieve the mean inferred reservoir temperature of 150°C would range from 4.5 to 5.7 km. A micro-earthquake survey run in the region for 30 days by Kumamoto (1978) suggests active, intense fracturing in the depth range 3-7 km indicating that channelways for this deep circulation of meteoric waters probably do exist. Unfortunately, no heat-flow measurements are available in the ranges surrounding the Black Rock Desert. Such data would provide useful information on the extent of the systems, location of recharge areas, and subsurface groundwater flow (Lachenbruch and others, 1976).

CONCLUSIONS

The heat-flow measurements made in this study, when combined with previous geological, geochemical and geophysical data lead to several conclusions which provide important constraints on the development of realistic geologic and thermal models for Black Rock Desert hydrothermal systems:

1) The nature (basaltic) and age (>20 m.y.) of volcanism in the region appear to preclude its being related to the heat source for modern activity suggesting that the hot springs are stable stationary phases supported by high regional heat flow and forced convection.

2) The net anomalous heat discharge from the hot spring systems is on the order of 30 MW based on estimates of convective and conductive heat loss. Heat transfer by moving groundwater in a "normal" Basin and Range heat-flow environment can easily provide the observed power loss.

3) Circulating groundwater flow from reasonably shallow depths ($\sim$2 to 6 km) can maintain the observed temperatures and mass discharges for hot springs in the Black Rock Desert.

4) Hot and warm springs occur on or very near faults with Quaternary displacements. Perhaps these are the only places where conduits exist through which water may rise to the surface. Conceivably hot water may come from depth in many other places along fracture zones, only to mix with cooler groundwater and leak into the alluvium before it can be discharged at the surface.

References

Bonham, H. F., 1969, Geology and mineral deposits of Washoe and Storey counties, Nevada: Nevada Bureau of Mines Bulletin, v. 70, 140 p.

Brook, C. A., Mariner, R. H., Mabey, D. R., Swanson, J. R., Guffanti, M., and Muffler, L. J. P., 1979, Hydrothermal convection systems with reservoir temperatures 90°C, in Assessment of Geothermal Resources of the United States, 1978, edited by L. J. P. Muffler: U.S. Geological Survey Circular 790, p. 18-85.

Crewdson, R. A., 1978, A gravity survey of Hualapi Flat and the southern part of the Black Rock Desert, Nevada: Colorado School of Mines Quarterly, v. 73, no. 3, p. 73-84.

Dodge, R. L., and Grose, L. T., 1979, Seismotectonic and geomorphic evolution of a typical Basin and Range normal fault, the Holocene Black Rock fault, northwestern Nevada: Geological Society of America, Abstracts with Programs, v. 11, no. 3, p. 75.

Grose, L. T., 1978, Late Quaternary tectonic controls of occurrence of geothermal systems in Gerlach-Hualapi Flat area, northwestern Nevada: Colorado School of Mines Quarterly, v. 73, no. 3, p. 11-14.

Grose, L. T., and Sperandio, R. J., 1978, Geology of the Gerlach-Hualapi Flat geothermal area, northwestern Nevada: Colorado School of Mines Quarterly, v. 73, no. 3, p. 1-10.

Keller, G. V., Grose, L. T., and Crewdson, R. A., 1978, Speculations on nature of geothermal energy in Basin and Range province of western United States: Colorado School of Mines Quarterly, v. 73, no. 4, p. 71-76.

Kumamoto, L., 1978, Microearthquake survey in the Gerlach-Fly Ranch area of northwestern Nevada: Colorado School of Mines Quarterly, v. 73, no. 3, p. 45-64.

Lachenbruch, A. H., and Sass, J. H., 1977, Heat flow in the United States and the thermal regime of the crust, in The Earth's Crust, edited by J. G. Heacock: American Geophysical Union Geophysical Monograph 20, p. 626-675.

Lachenbruch, A. H., Sorey, M. L., Lewis, R. E., and Sass, J. H., 1976, The near-surface hydrothermal regime of Long Valley caldera: Journal of Geophysical Research, v. 81, p. 763-768.

Lachenbruch, A. H., and Sass, J. H., 1978, Models of an extending lithosphere and heat flow in the Basin and Range province: Geological Society of America Memoir 152, p. 209-250.

Mase, C. W., Chapman, D. S., and Ward, S. H., 1978, Geophysical study of the Monroe-Red Hill Geothermal System: University of Utah Topical Report IDO/76-1601-77-17, 89 p.

Olmsted, F. H., Glancy, P. A., Harrill, J. R., Rush, F. E., and VanDenburgh, A. S., 1975, Preliminary hydrogeologic appraisal of selected hydrothermal systems in northern and central Nevada: U.S. Geological Survey Open-File Report 75-56, 267 p.

Renner, J. L., White, D. E., and Williams, D. L., 1975, Hydrothermal convection systems, in Assessment of Geothermal Resources of the United States, 1975, edited by D. E. White and D. L. Williams: U.S. Geological Survey Circular 726, p. 5-57.

Sass, J. H., Blackwell, D. D., Chapman, D. S., Costain, J. K., Decker, E. R., Lawver, L. A., and Swanberg, C. A., 1980, Heat flow from the crust of the United States, in Touloukian, Y. S., Judd, W. R., and Roy, R. F., eds., Physical Properties of Rocks and Minerals: McGraw-Hill Book Company, in press.

Sass, J. H., Lachenbruch, A. H., Munroe, R. J., Greene, G. W., and Moses, T. H., Jr., 1971, Heat flow in the western United States: Journal of Geophysical Research, v. 76, p. 6376-6413.

Sass, J. H., Zoback, M. L., and Galanis, S. P., Jr., 1979, Heat flow in relation to hydrothermal activity in the southern Black Rock Desert, Nevada: U.S. Geological Survey Open-File Report 79-1467.

Schaefer, D. H., Welch, A. H., and Douglas, K. M., 1980, Studies of the geothermal potential of the western arm of the Black Rock Desert, northwestern Nevada: U.S. Geological Survey Open-File Report, in preparation.

Sorey, M. L., 1975, Numerical modeling of liquid geothermal systems: U.S. Geological Survey Open-File Report 75-613.

Ward, S. H., Parry, W. T., Nash, W. P., Sill, W. R., Cook, K. L., Smith, R. B., Chapman, D. S., Brown, F. H., Whelan, J. A., and Bowman, J. R., 1978, A summary of the geology, geochemistry, and geophysics of the Roosevelt Hot Springs thermal area, Utah: Geophysics, v. 43, no. 7, p. 1515-1542.

Waring, G. A., 1975, Thermal springs of the United States and other countries of the world: U.S. Geological Survey Professional Paper 492.

Wilden, R., 1964, Geology and mineral deposits of Humboldt County, Nevada: Nevada Bureau of Mines Bulletin, v. 59, 154 p.

Zeisloft, T. J., and Keller, G. V., 1978, Magnetotelluric survey across Black Rock Desert-Hualapi Flat area, Nevada: Colorado School of Mines Quarterly, v. 73, no. 4, p. 39-46.

Zoback, Mary Lou, and Thompson, G. A., 1978, Basin and Range rifting in northern Nevada--Clues from a mid-Miocene rift and its subsequent offsets: Geology, v. 6, p. 111-116.

APPENDIX: Temperature Measurements

The boreholes were drilled during the summer of 1979. Temperatures were obtained at 0.3 m intervals for all boreholes in October 1979, by which time all temperature disturbances introduced by the drilling process should have subsided. Temperature profiles are presented graphically in Figures 6 through 17. A smoothed average temperature gradient over 3-m intervals is also shown on each of these figures. The high frequency excursions in temperature profiles for boreholes BR10 and BR11 (Figures 15 and 16) are attributed to the presence of gas bubbles observed streaming from the boreholes during the logging operations.

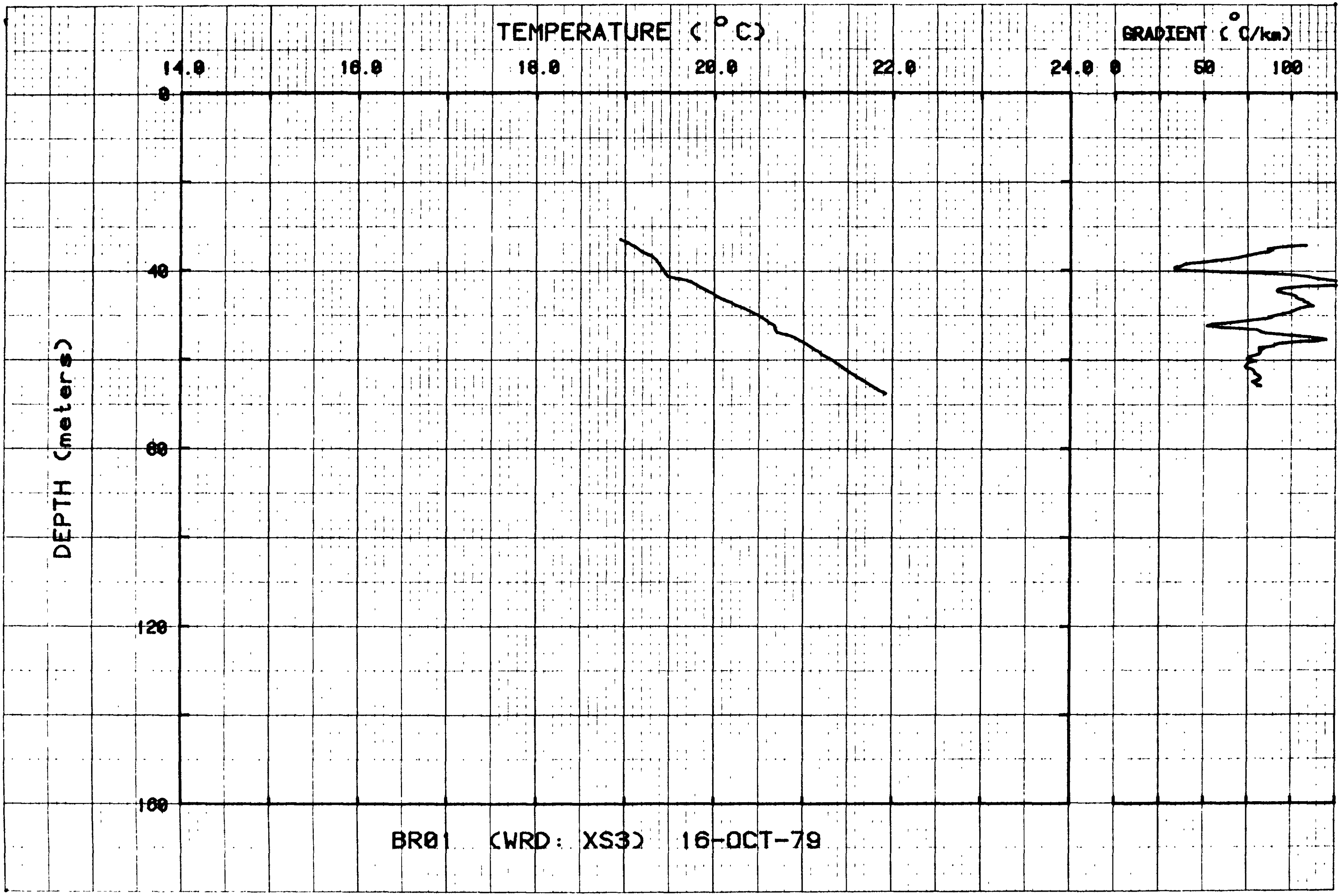

Figure 6. Temperature and gradients for borehole BR01.

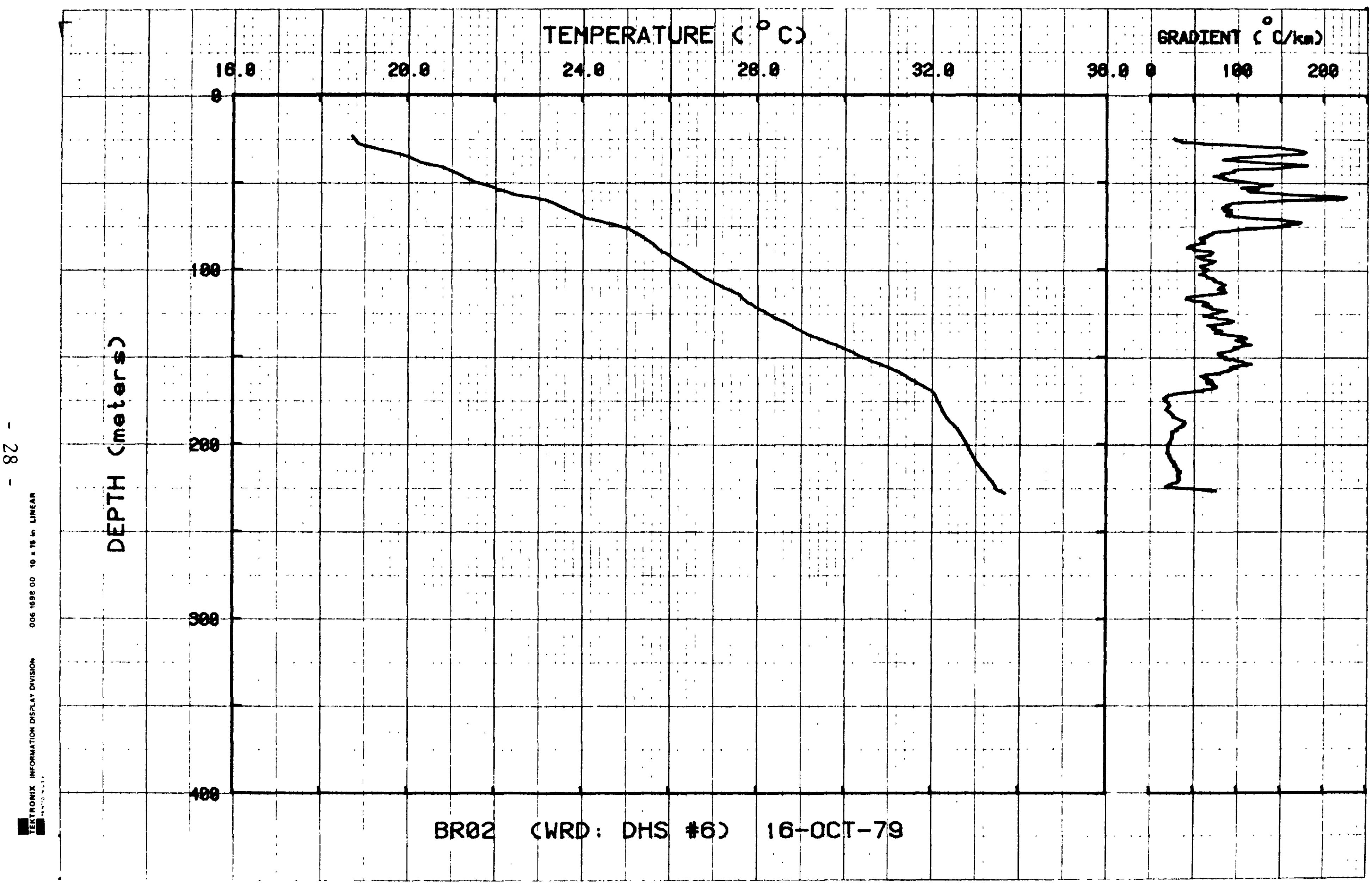

Figure 7. Temperature and gradients for borehole BR02.

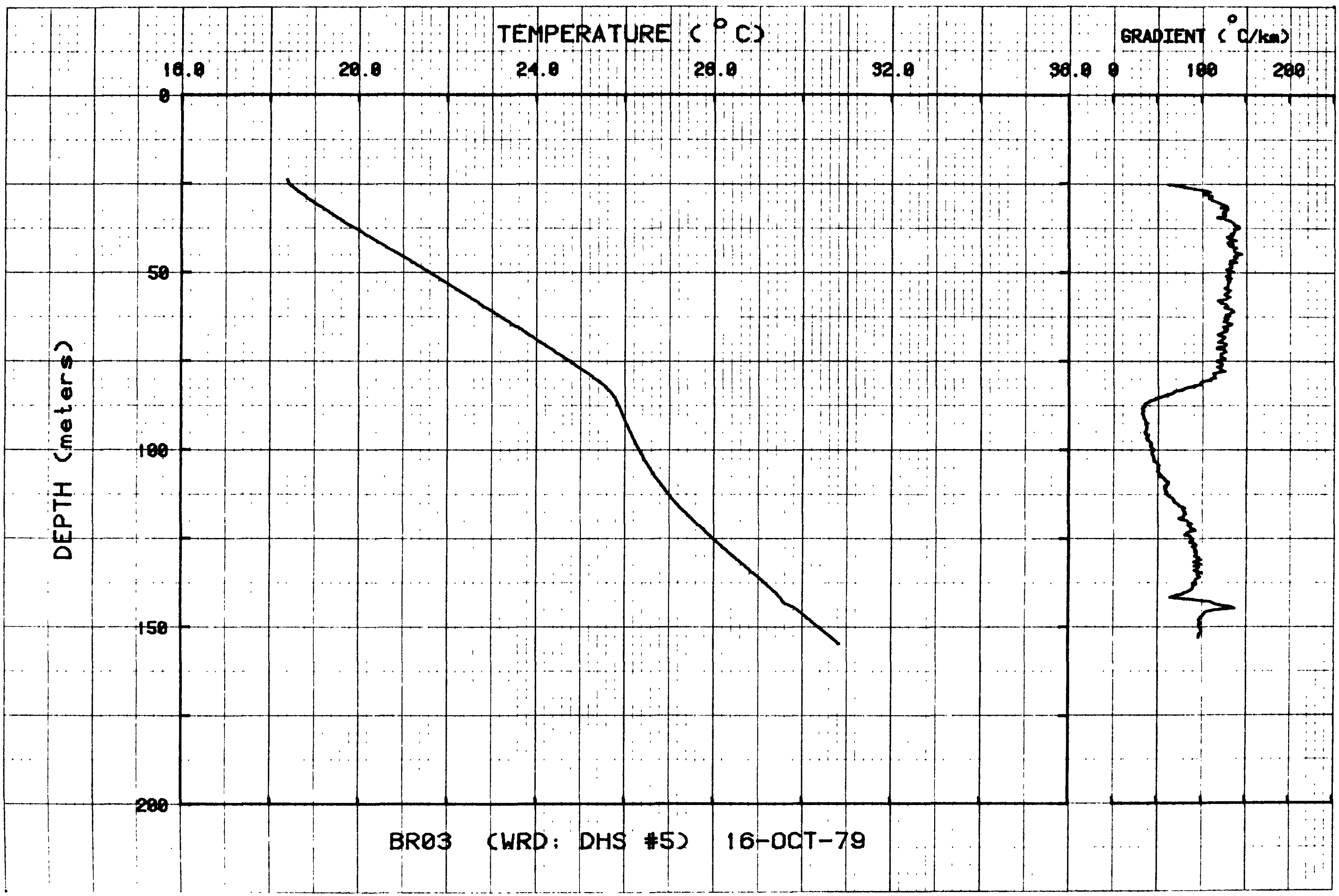

Figure 8. Temperature and gradients for borehole BR03.

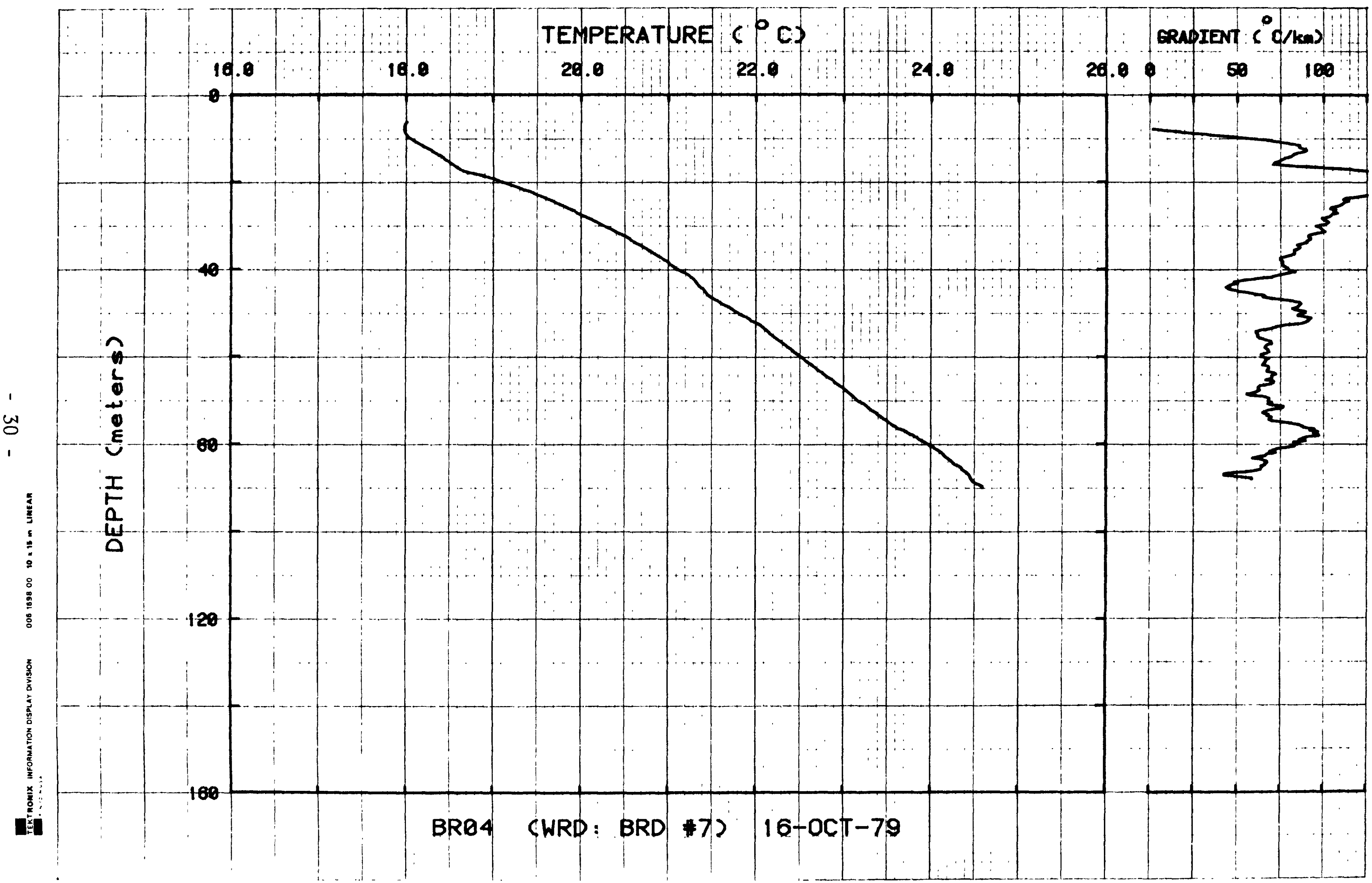

Figure 9. Temperature and gradients for borehole BR04.

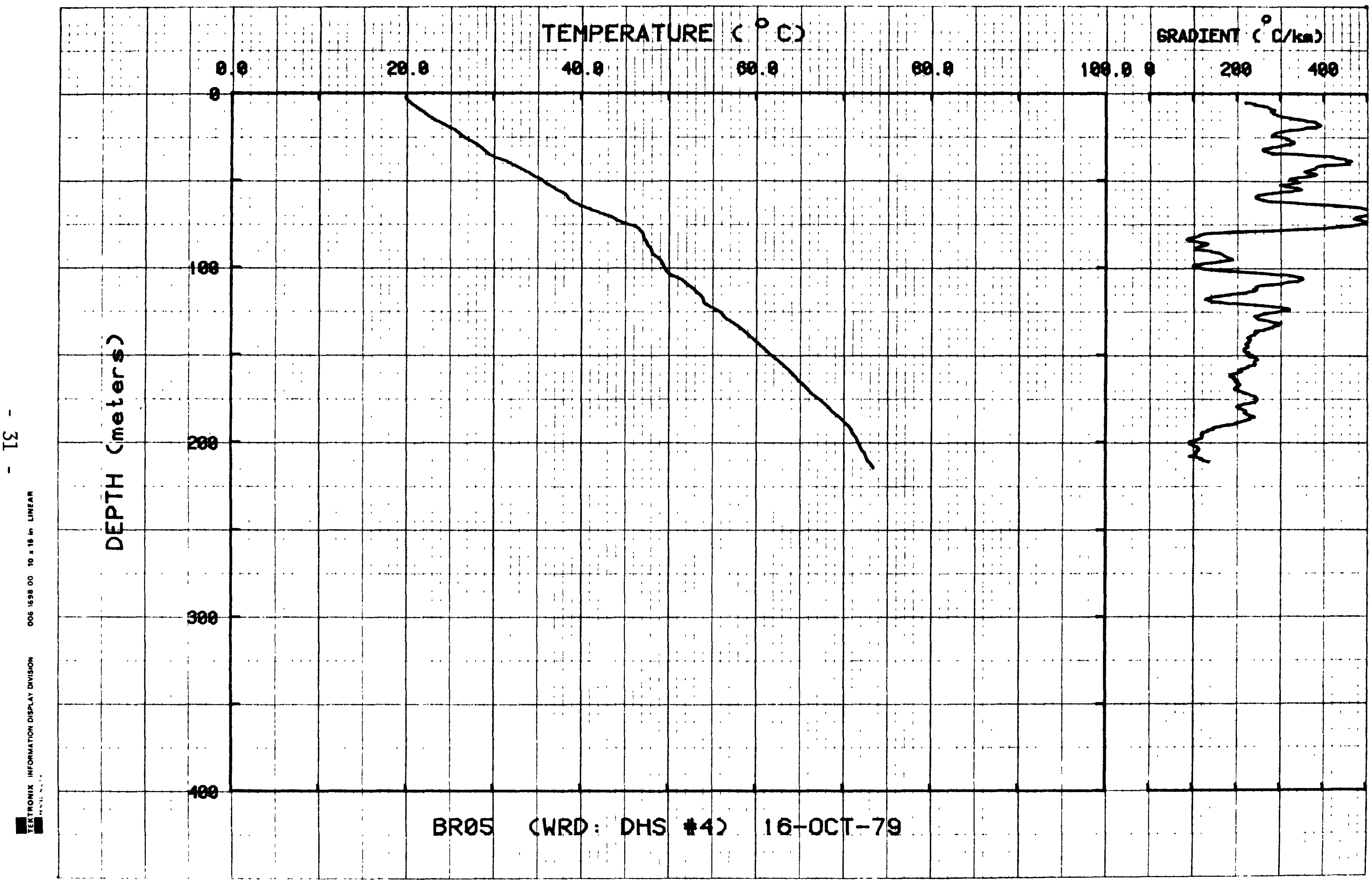

Figure 10. Temperature and gradients for borehole BR05.

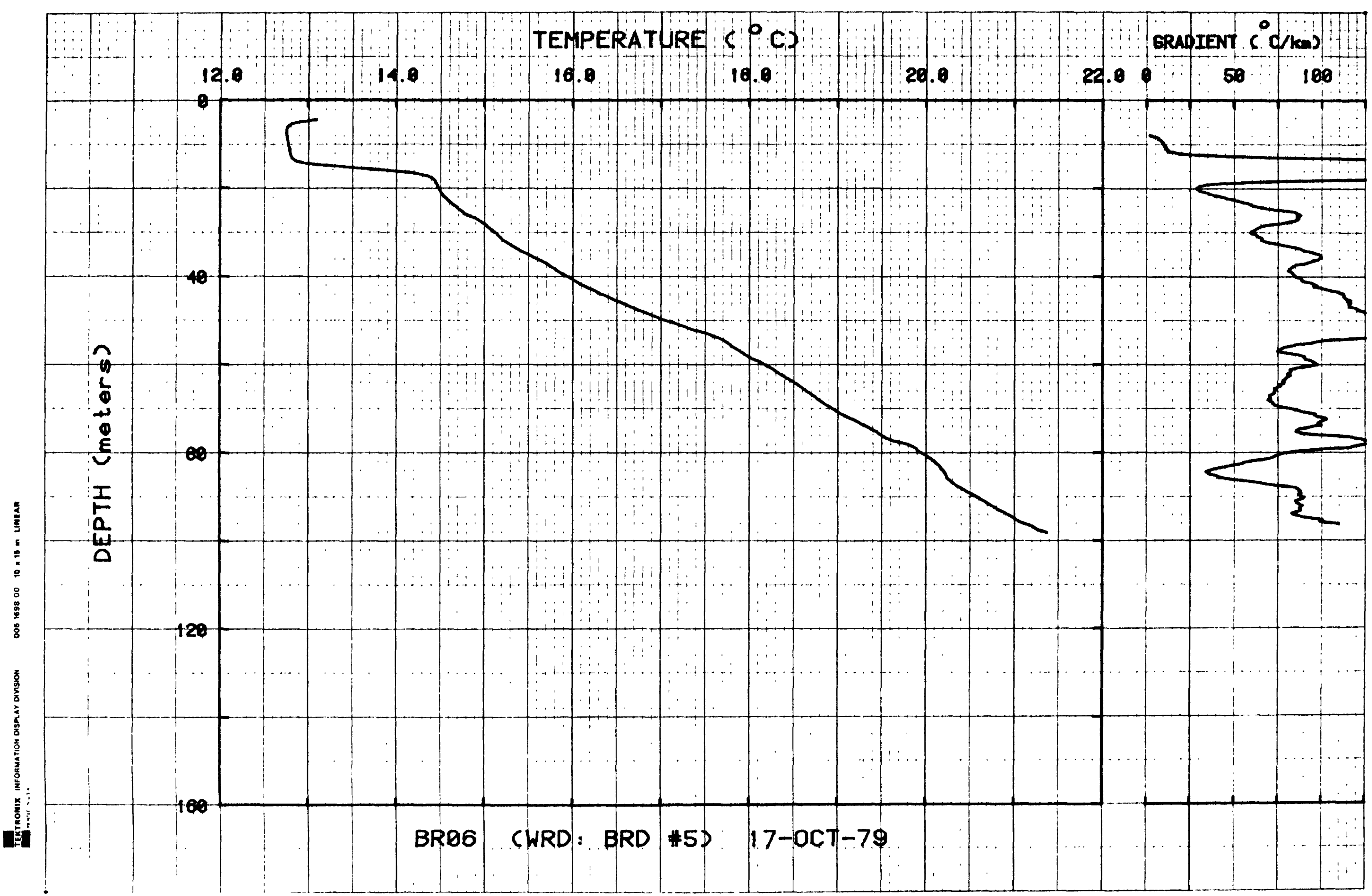

Figure 11. Temperature and gradients for borehole BR06.

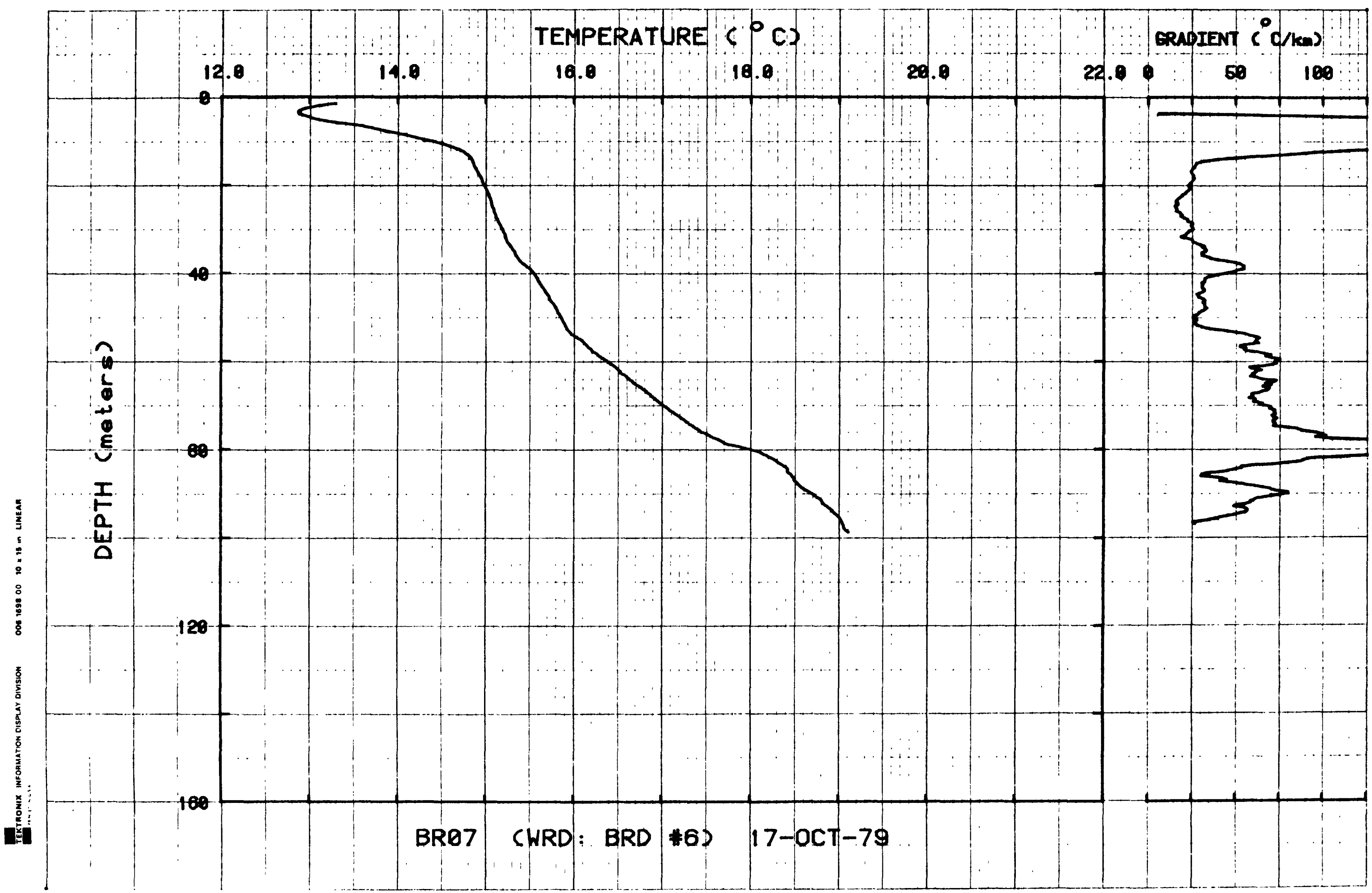

Figure 12. Temperature and gradients for borehole BR07.

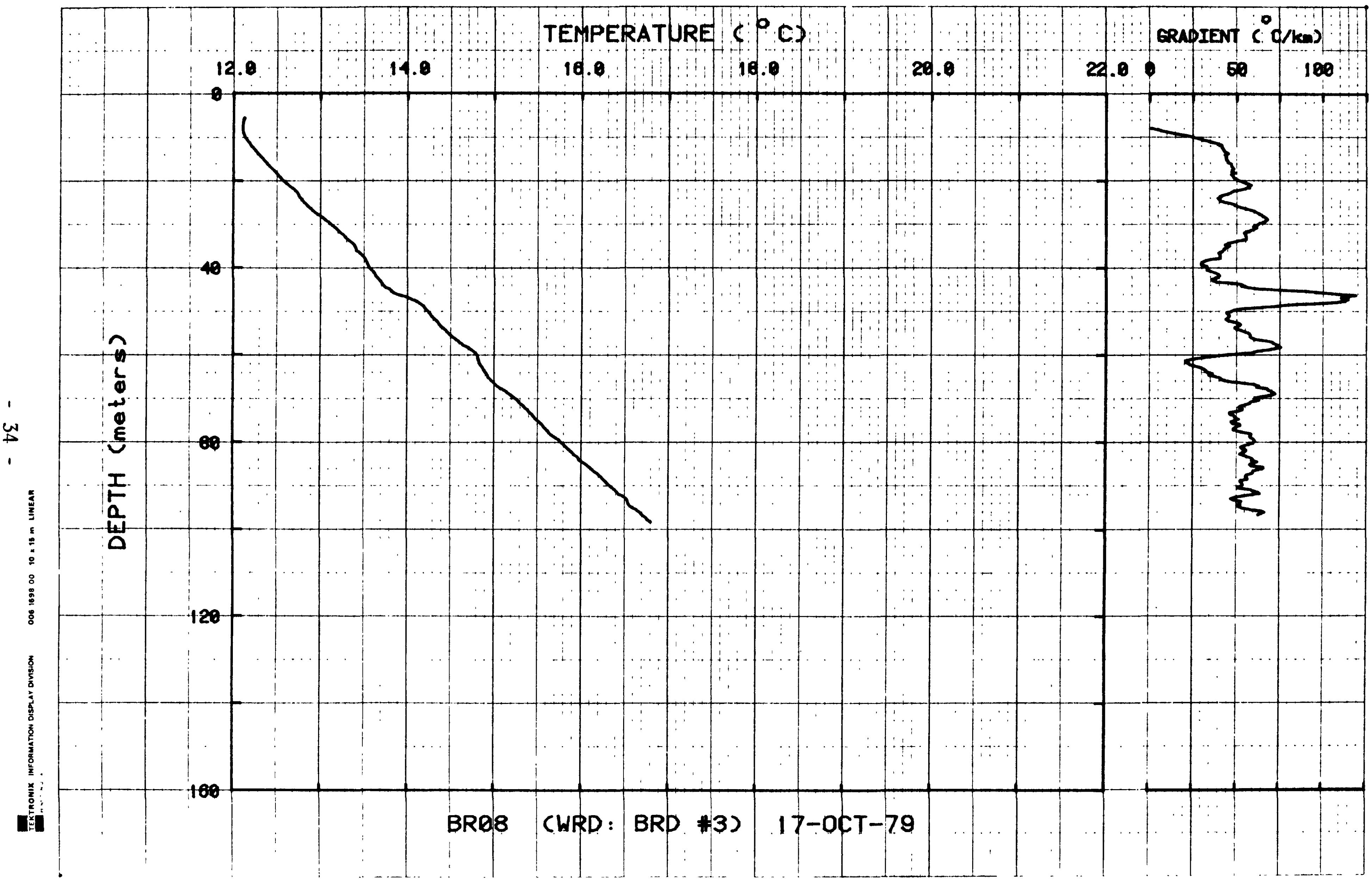

Figure 13. Temperature and gradients for borehole BR08.

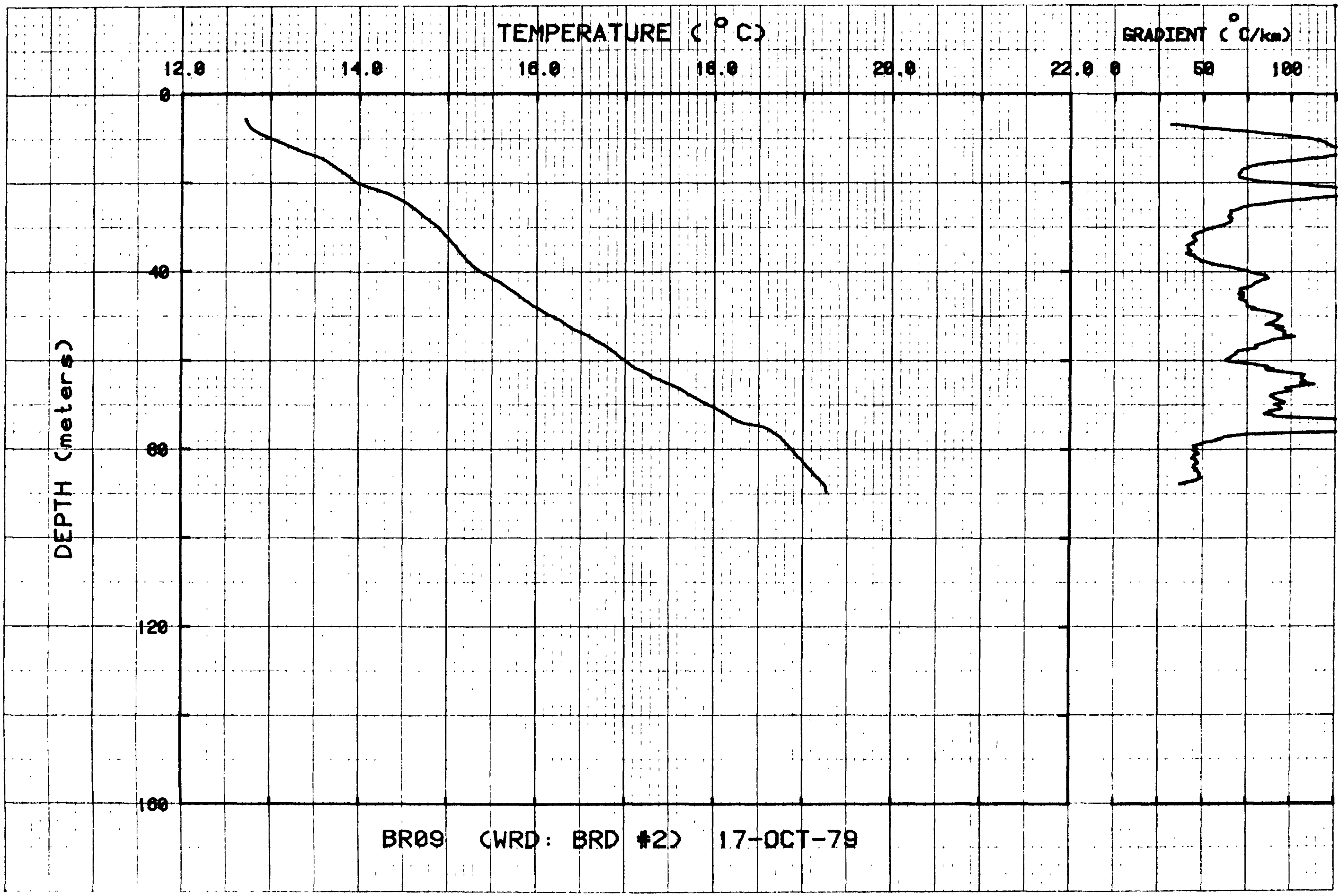

Figure 14. Temperature and gradients for borehole BR09.

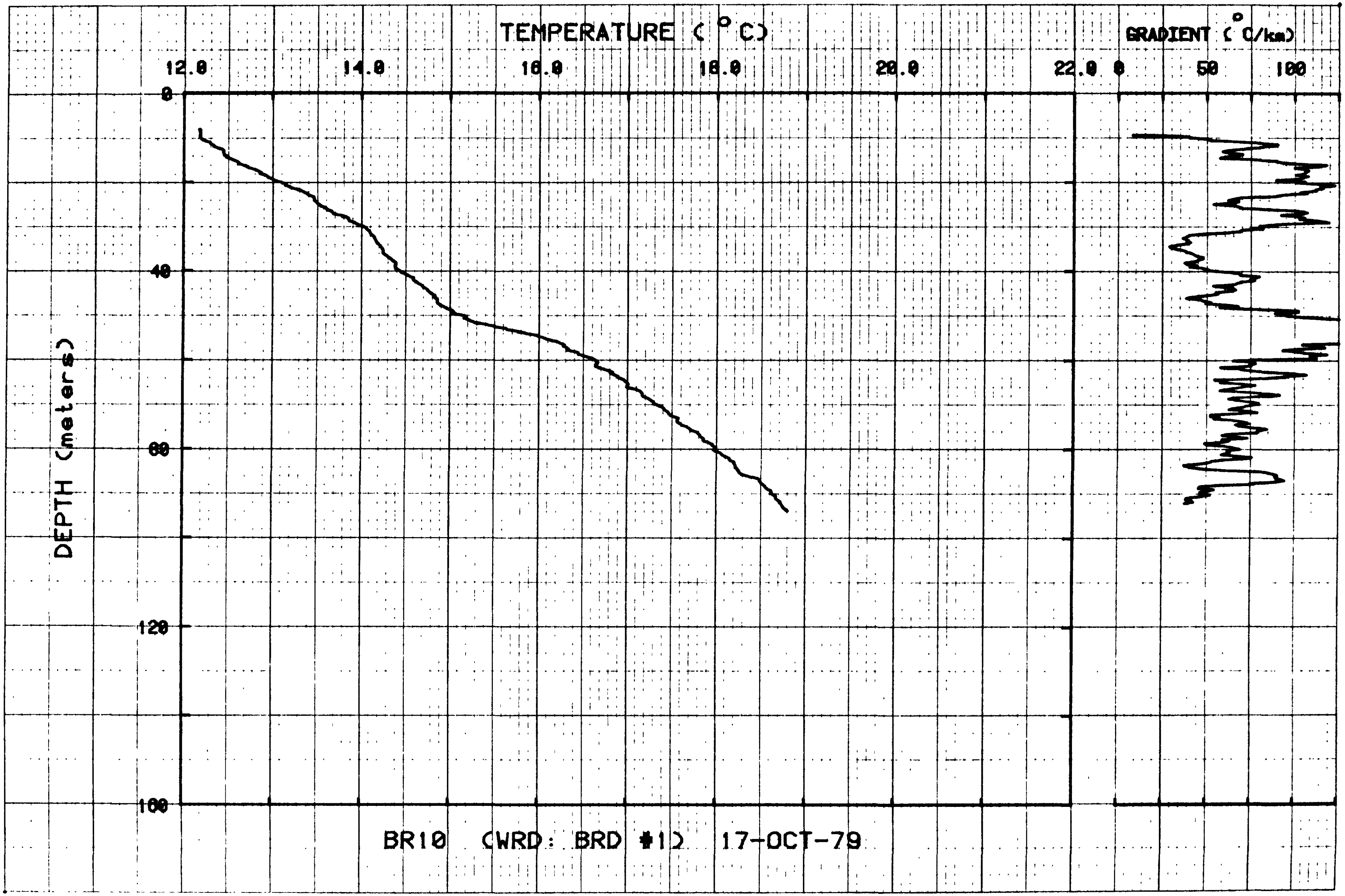

Figure 15. Temperature and gradients for borehole BR10.

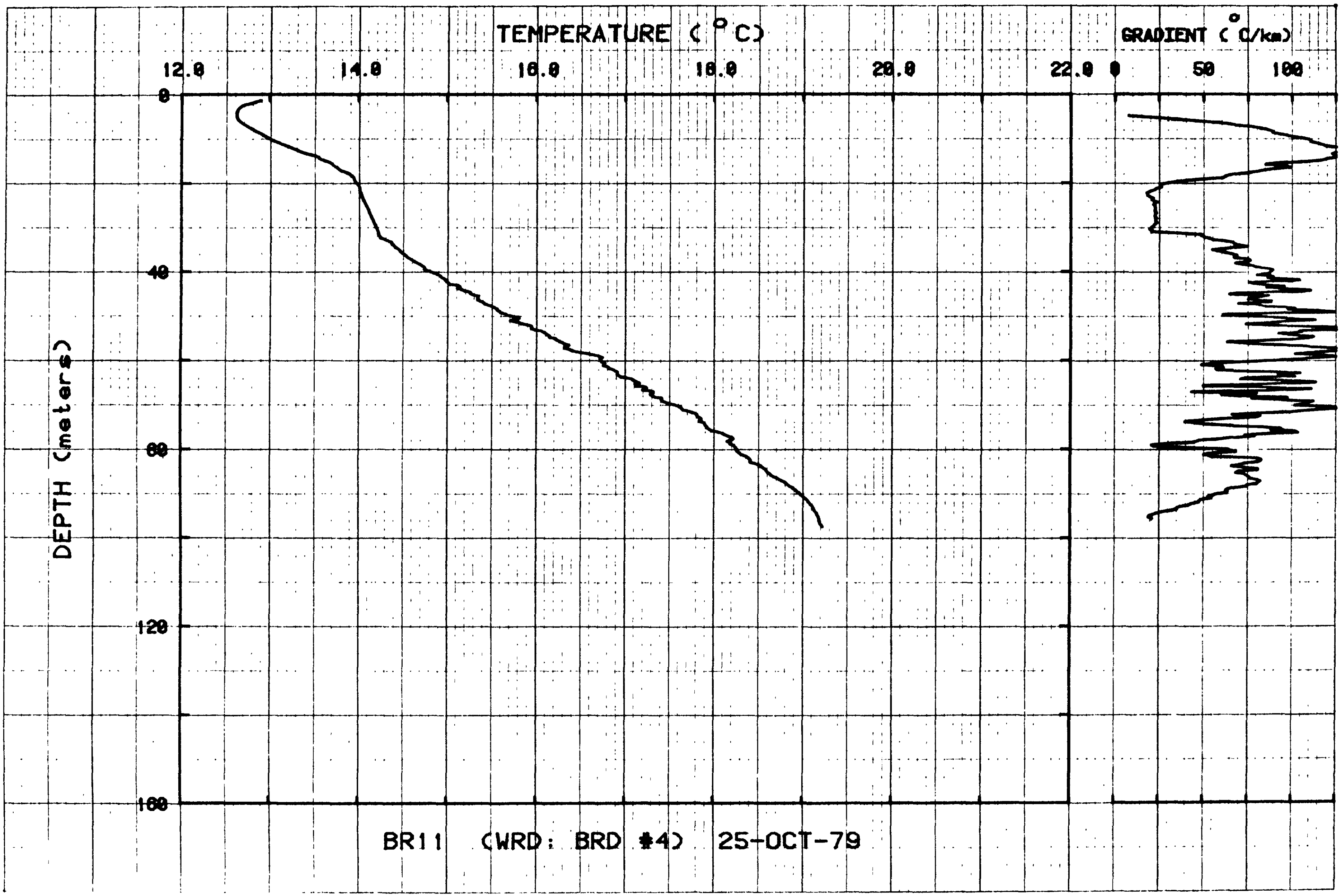

Figure 16. Temperature and gradients for borehole BR11.

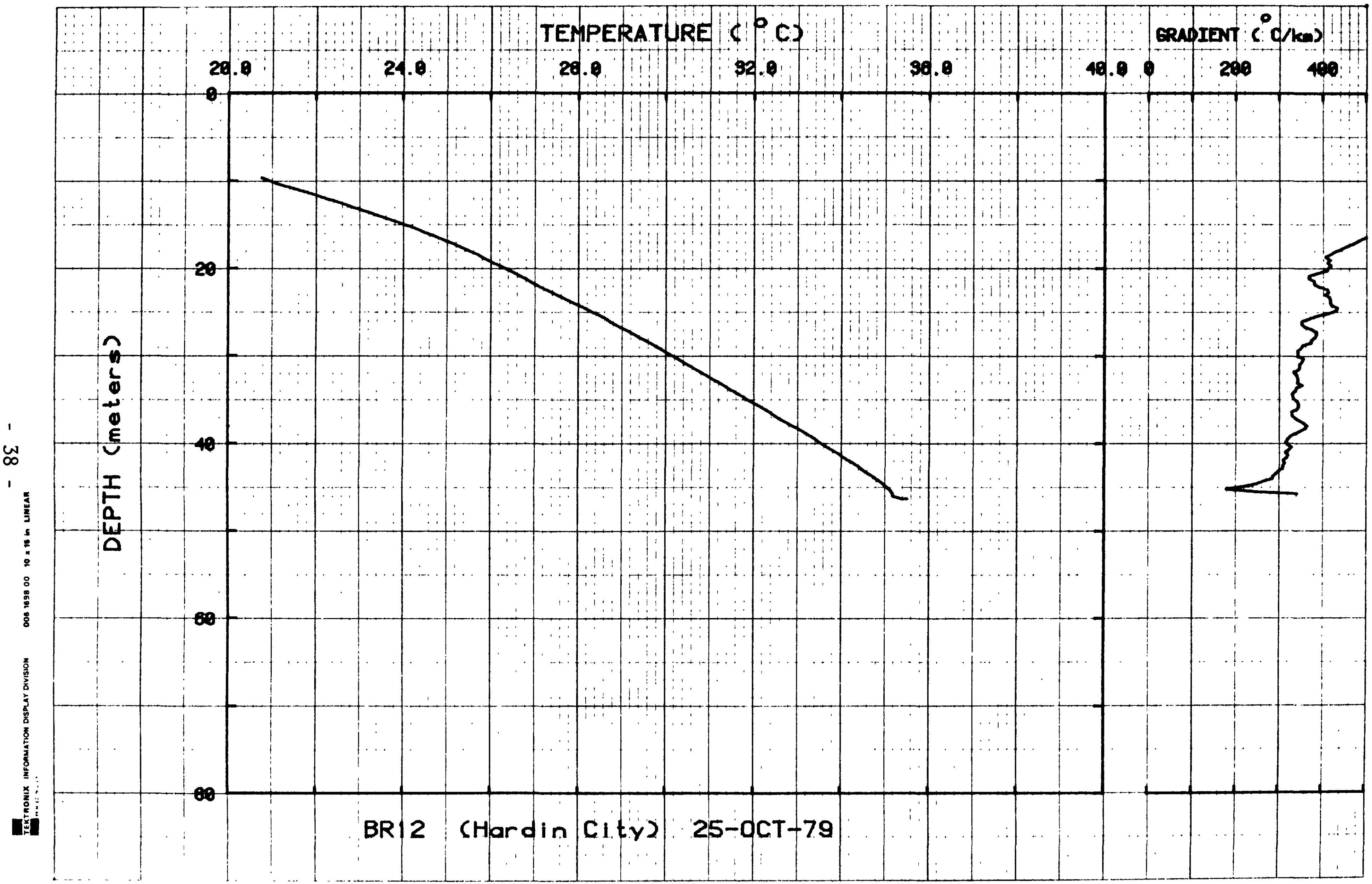

Figure 17. Temperature and gradients for borehole BR12.